Relationship between structure and reactivity of carbonaceous materials

A. Arenillas, F. Rubiera, C. Pevida, C.O. Ania and J.J. Pis

Instituto Nacional del Carbón, CSIC, Apartado 73, 33080 Oviedo, SPAIN

Abstract

Knowledge of the amount and distribution of active sites in carbons is of paramount importance for a better understanding of the kinetics involved in heterogeneous gas-solid reactions. In this work a commercial active carbon, CM, was treated at several temperatures in order to obtain a series of samples with different textural and structural properties. The results showed that the loss of reactivity of the samples, determined by thermogravimetric analysis, is related not only to the lower surface area but also to the decrease in the amount of active sites due to a higher structural ordering.

Keywords: Thermal analysis, reactivity, adsorption, chemisorption, structural ordering, active carbon.

1. INTRODUCTION

In the heterogeneous reactions between gases and carbon, the rate of reaction is generally assumed to be proportional to the accessible surface area of the solid. However, it has long been recognised that the reactivity of carbonaceous materials is related not only to the surface area but also to surface accessibility, carbon active sites (edges, basal plane defects, heteroatoms) and catalytic active sites created by natural inorganic impurities or dopents [1-2]. Thus, these carbon active sites constitute the so-called active surface area (ASA), which only comprises a fraction of the total surface area. Knowledge of the nature and concentration of the active sites is of paramount importance for a better understanding of the kinetics involved in heterogeneous gas-solid reactions [3].

There is, however, some controversy regarding the ASA values and their relationship with carbon reactivity, for several reasons. First, oxygen chemisorption used for the evaluation of ASA depends on the operating conditions (i.e., time, temperature, oxygen partial pressure) [4-5]. Even when the same operating conditions are employed, different ASA values are obtained with different methods [6-7]. Furthermore, each researcher has proposed that the reactivity is proportional to the ASA measured by his own method, although ASA is usually measured at temperatures lower than the reaction temperature [8]. Nevertheless, it seems to be clear that the differences in reactivity of carbons can be ascribed to the fact that different carbons have *initially* different ASA [9-10] and, thus, the amount of chemisorbed oxygen can be related to the reactivity of carbon materials.

The increase in heat treatment temperature (HTT) results in a substantial reactivity reduction, associated with major changes of the turbostratic carbon structure [11], and thus with variation in the amount and/or accessibility of active sites.

Thermogravimetric analysis has been extensively used for the reactivity characterisation of different materials, and for the study of different heterogeneous reactions involving carbonaceous samples [12, 13]. Although extrapolation to other systems at larger scale cannot be directly performed, thermogravimetric analysis is very useful from a fundamental viewpoint, and for comparison between samples treated under different conditions. The isothermal reactivity at low temperatures is widely applied for characterising the reactivity of carbonaceous materials in order to predict their behaviour at higher temperatures, and to evaluate the relevance of the annealing that has taken place after treating the samples at high HTT. The well controlled operating conditions and relatively low time consuming of these analyses provide further advantages.

In this work, thermogravimetric techniques were used in order to evaluate the amount of active sites in carbon materials and to follow their variation in reactivity with the increase in

heat treatment temperature. Furthermore, the reactivity of the samples was related to their active surface area, textural and structural properties.

2. EXPERIMENTAL

An activated carbon (denoted as CM) was treated in a graphite furnace (Pyrox VI 150/25) at several temperatures under inert atmosphere in order to obtain a series of samples with different textural and structural properties. The samples were heated at 20 ºC min^{-1} from room temperature to 1400, 1800, 2000, 2200 and 2400 ºC, and maintained at the final temperature during 2 hours. The samples were denoted as CM-1400, CM-1800, CM-2000, CM-2200 and CM-2400, respectively, and their chemical analyses are presented in Table 1.

The textural characterisation of the samples studied was carried out by physical adsorption of N_2 at -196 ºC. The BET surface areas and pore volumes of the samples are presented in Table 2.

The active surface area (ASA) was determined by temperature programmed desorption tests (TPD) in a thermogravimetric analyser. In order to minimise diffusion problems and secondary reactions of the desorbed CO and/or CO_2 with the solid material, 5 mg of sample and a gas flow rate of 75 mL min^{-1} were used. The samples were outgassed by heating in a stream of dry argon at 15 ºC min^{-1} up to 1000 ºC, and held at this temperature for 5 hours. Subsequently, the temperature was lowered to a previously optimised temperature of 250 ºC [7]. This temperature was chosen so that equilibrium could be achieved in a reasonable period of time, and simultaneous carbon gasification could be avoided. Once the temperature (250 ºC) was reached, the inert flow was changed to oxygen for 17 hours.

After the chemisorption step, the oxygen was swept by flowing argon, and a TPD test was performed in the thermogravimetric analyser (TGA) by heating the sample at 15 ºC min^{-1} from room temperature to 1000 ºC. The desorbed gases (CO and CO_2) were followed by

means of a mass spectrometer, and they were related to the amount of oxygen chemisorbed after calibration with calcium oxalate [14]. Figure 1 shows the relationships between the theoretical amount of CO and CO_2 produced from calcium oxalate decomposition and the experimental peak area values from the CO and CO_2 evolution profiles during the calibration tests (peak area values expressed in units of A A^{-1} min, where A is the measured intensity of CO or CO_2 in Amperes, normalised by the total intensity measured by the mass spectrometer). The ASA values (m^2 g^{-1}) presented in Table 2 were calculated using the equation:

$$ASA = \frac{N_O \sigma_O N_{avo}}{w}$$

where σ_O is the cross-sectional area of the oxygen atom (0.083 nm^2 [10]), N_{avo} is the Avogadro constant and w is the mass of the carbon material in grams. The number of moles of chemisorbed oxygen, N_O, was obtained from the amount of oxygen desorbed during the TPD tests.

The samples were crystallographically characterised by means of X-ray diffraction analysis (XRD). The diffractograms were recorded using Cu Kα radiation (λ=0.15406 nm) at a step size of 0.02º.

Isothermal reactivity tests (500 ºC) under 20% oxygen in argon were conducted in a thermogravimetric analyser. In order to compare the samples, factors such as sample mass and gas flow rate need to be well established to ensure good repeatability between experimental runs. In this work, 5 mg of sample and a gas flow rate of 50 mL min^{-1} were employed.

3. RESULTS AND DISCUSSION

As can be observed in Table 1, except for the initial sample, CM, all the treated samples contain mainly carbon in their composition, with very low amounts of heteroatoms. The increase in the HTT produces a loss of labile functional groups that is reflected in their

chemical composition and textural properties. Figure 2 presents the linear relationship found between the HTT and the BET area values for the samples studied. As the severity of treatment conditions increases (i.e., higher temperature) the apparent BET surface area and pore volume, determined by N_2 adsorption, show a significant decrease from 1587 m^2g^{-1} to 146 m^2g^{-1} for samples CM and CM-2400, respectively (see Table 2).

The decrease in BET area values with the increase in treatment temperature could be due to condensation of the turbostratic structure (i.e., hydrogen loss, edge coalescence, defect elimination) and the consequent increase in the ordering of the samples studied [2]. Although more work is needed to understand the mechanisms involving thermal annealing, it has been associated with structural ordering of the carbon on a molecular level and micropore collapse [15] with the corresponding decrease in surface area values. The XRD analysis corroborates this assumption. Figure 3 presents the X-ray intensity curves for the samples. Peaks at around 26º correspond to the (002) reflection of carbon resulting from the stacking structure of aromatic layers. The two dimensional (10) band at $2\theta = 43º$ arises from graphite-like atomic order within a single plane. As the temperature increases the (002) peak becomes narrower. This can be interpreted in terms of crystallites with larger dimensions. During the first stages of gasification and/or combustion processes, the crystallites or the so-called carbon turbostratic structure would develop gradually as a result of the high temperature, making the carbon structure more ordered and compact. This is called carbon crystallisation or crystallite growth that would decrease the reactivity of the material [16].

From the XRD patterns presented in Figure 3, typical crystallographic parameters (i.e., pseudographitic interplanar spacing, d_{002}; width of the crystal or layer of graphitic planes, La; and height of these planes, Lc) can be deduced. Table 3 shows the values of these parameters for the samples studied. It can be observed that the temperature of treatment mainly affects the size of the planes (i.e., La and Lc). The increase of La and Lc with HTT could be

attributed to one or more processes: in plane crystallite growth, coalescence of crystallites along the c-axis and coalescence of crystallites along the a-axis, depending on the temperature range [17]. The higher the treatment temperature the higher the size of the graphitic planes, and the lower the content of amorphous carbon that remains [15]. However, the interplanar spacing, d_{002}, of the samples studied is almost constant.

The isothermal (500 ºC) reactivity of the samples was determined in the TGA system. The burn-off profiles are presented in Figure 4. It can be seen that as the temperature increases, the samples become less reactive. This is due to the increase in the degree of structural ordering with temperature, already mentioned, with associated loss of free electrons. A relatively simple reaction as the one occurring during carbon gasification and/or combustion can be described by several elementary steps [18]:

$$2 * + O_2 \rightarrow O_2 ads \quad (1)$$

$$O_2 ads + 2e^- \rightarrow {O_2}^{2-} ads \quad (2)$$

$$O2^{2-} ads + 2e^- \rightarrow 2O^{2-} ads \quad (3)$$

$$C\# + O^{2-} ads \rightarrow COads + 2e^- + * \quad (4)$$

$$COads \rightarrow CO + C\# \quad (5)$$

$$COads + O^{2-} ads \rightarrow CO_2 ads + 2e^- + * \quad (6)$$

$$CO_2 ads \rightarrow CO_2 + C\# \quad (7)$$

Besides the reaction centre (C#), a second type of chemisorption site (*) is required for the reductive activation of oxygen, which must exhibit an excess of delocalised electrons. The increase in condensation degree is reflected by a decrease in the ratio of edge (more reactive) to basal carbon atoms due to the increase in the diameter of the crystallite [11]. It is therefore clear that the higher the treatment temperature, the lower the amount of active sites and delocalised electrons available, and thus the lower the reactivity to oxygen.

In most of the typical normalised TGA reactivity plots an induction period was observed. As reported elsewhere [19] this initial part of the burn-off curve with an increasing slope is due to opening of the previously closed pores and a balance between mass gain due to stable complex formation and mass loss due to carbon gasification [20]. From the isothermal (500 ºC) reactivity tests obtained in this work, the initial reactivity of the samples at X = 0, R_0, was estimated by extrapolation from the burn-off curve after the induction period mentioned above.

A series of parameters such as available surface area, amount of active sites (i.e., ASA values), structural ordering (i.e., crystallographic parameters) and the reactivity of the samples are *a priori* interconnected. Figure 5 shows the relationships between R_0 and textural properties (BET area and pore volume determined by N_2 adsorption). It can be observed that, at least with the samples studied in this work, there is a very good linear relationship between R_0 and textural properties. However, this could be due to the pore size distribution in the samples studied. Good correlations are usually found between surface area and reactivity under chemical control, but not in the case of carbon materials with morphological restrictions, such as microporous carbons [9]. In the latter case it has been observed that samples may present slight differences in surface area values but quite big differences in reactivity [21, 22]. Thus, the use of textural parameters as the only indicators of the reactive behaviour of carbonaceous samples can be misleading.

Figure 6 shows the relationship between R_0 and crystallographic parameters, determined from XRD analysis. The La and Lc values give an idea of the ordering and deactivation degree of the samples, which are directly correlated with the amount of active sites that remain available. It can be seen in Figure 6 that there is also a linear relationship between those crystallographic parameters and R_0.

Figure 7 presents the relationship between R_0 and active surface area. It can be seen that the ASA values and R_0 of the samples present a linear relationship. The estimated reactivity, R_0, can be converted into values per unit of surface area of the sample [9, 23]. In this work, the normalised R_0 values in terms of surface area determined by nitrogen physical adsorption will be denoted as specific reactivity, R_S. The R_0 values normalised with active surface areas evaluated from oxygen chemisorption will be named as intrinsic reactivity, R_i.

$$R_S = R_0 / BET \quad (8)$$

$$R_i = R_0 / ASA \quad (9)$$

Figure 8 shows the evolution of the different reactivity values with the treatment temperature. It can be seen that R_0 decreases with an increase in the temperature of treatment, as was expected, due to the annealing effect. The ASA values also decrease with an increase of HTT (see Table 2), and the extent of this decrease makes that R_i follows the same behaviour that R_0 with HTT, although R_0 decreases nearly four times and R_i only decreases by a factor of 1.7 between 1400 and 2400 ºC. However, R_S remains nearly constant. This implies that despite the fact that the large decrease in apparent surface area with the increase of HTT (see Figure 2) is a factor in explaining the decrease in char reactivity, other factors such as the availability of active sites exerts the greatest effect in the variation of the samples intrinsic reactivity.

4. CONCLUSIONS

The results obtained for the samples studied in this work indicate that an increase in the heat treatment temperature causes a substantial decrease in BET surface area as well as the loss of active sites, as indicated by the decrease in the ASA values determined in the TGA.

The lower reactivity of the samples to oxygen is due to the structural changes that they have experienced during heat treatment, resulting in their thermal deactivation. The estimated

initial reactivity presents a linear relationship with BET surface area, ASA, and crystallite structure of the samples (La and Lc, determined by XRD analysis). The results confirmed that apparent BET surface area is not a relevant reactivity normalisation parameter; active surface area appears to be a fundamental parameter that better indicates the variation of samples reactivity.

References

[1] J.T. Ashu, N.Y. Nsakala, O.P. Mahajan, P.L. Walker Jr. Fuel 57 (1978) 250.

[2] R.H. Hurt. 27th Symp. (Int) Comb./The Comb. Institute (1998) 2887.

[3] P. Ehrburger, F. Louys, J. Lahaye. Carbon 27 (1989) 389.

[4] H. Teng, C.T. Hsieh. Ind. Eng. Chem. Res. 38 (1999) 292.

[5] J. Lahaye, J. Dentzer, P. Soulard, P. Ehrburger. Fundamental issues in control of carbon gasification reactivity, Kluwer Academic Press, Netherlands 1991, p. 143.

[6] A. Arenillas, F. Rubiera, J.B. Parra, J.J. Pis. Carbon 40 (2002) 1381.

[7] A. Arenillas, F. Rubiera, J.B. Parra, J.J. Pis. Studies in Surface Science and Catalysis 144 (2002) 209.

[8] K. Miura, K. Hashimoto, P.L. Silveston. Fuel 68 (1989) 1461.

[9] C.V. Guterl, G. Bekri, J. Dentzer, S. Manocha, L.M. Manocha, P. Ehrburger. J. Anal. Appl. Pyr. 67 (2003) 341.

[10] N.R. Laine, J. Vastola, P.L. Walker Jr. J. Phys. Chem. 67 (1963) 2030.

[11] O. Senneca, P. Russo, P. Salatino, S. Masi. Carbon 35 (1997) 141.

[12] K.E. Ozbas, M.V. Kök, C. Hicylmaz. J. of Thermal Analysis and Calorimetry 69 (2002) 541.

[13] S. Kizgut, Y. Baran, D. Cuhadaroglu. J. of Thermal Analysis and Calorimetry 71 (2003) 857.

[14] P. Causton, B. McEnaney. Fuel 64 (1985) 1447.

[15] L. Lu, C. Kong, V. Sahajwalla, D. Harris. Fuel 81 (2002) 1215.

[16] X. Xu, Q. Chen, H. Fan. Fuel 82 (2003) 853.

[17] B. Feng, S.K. Bhatia, J.C. Barry. Carbon 40 (2002) 481.

[18] D. Herein, J. Find, B. Herzog, H. Kollmann, R. Schmidt, R. Schlögl, H. Bartl, C. Troyer. Prep. ACS, Div. Fuel Chem. 41 (1996) 148.

[19] L.R. Radovic, P.L. Walker Jr, R.G. Jenkins. Fuel 62 (1983) 849.

[20] A.A. Lizzio, A. Riotrowski, L.R. Radovic. Fuel 67 (1988) 1691.

[21] A. Arenillas, C. Pevida, F. Rubiera, J.J. Pis. Fuel 82 (2003) 2001.

[22] C. Pevida, A. Arenillas, F. Rubiera, J.B. Parra, J.J. Pis. Proceedings CARBON'02, Ed. Z. Dong, W. Zhong-Ze (2002).

[23] M.L. Chan, J.M. Jones, M. Pourkashanian, A. Williams. Fuel 78 (1999) 1539.

Table 1. Chemical analysis of the samples studied

	Ultimate analysis (wt% daf)				
Sample	C	H	N	S	O
CM	91.2	2.2	0.2	0.1	6.3
CM-1400	99.4	0.1	0.1	0.1	0.3
CM-1800	99.6	0.1	0.0	0.1	0.2
CM-2000	99.8	0.0	0.0	0.1	0.1
CM-2200	99.8	0.0	0.0	0.1	0.1
CM-2400	99.8	0.0	0.0	0.1	0.1

Table 2. Textural parameters of the carbon samples

	CM	CM-1400	CM-1800	CM-2000	CM-2200	CM-2400
Helium density (g cm^{-3})	1.68	2.10	1.80	1.65	1.44	1.35
BET Area ($m^2 g^{-1}$)	1587	761	534	385	212	146
Vp (N_2, $cm^3 g^{-1}$)	0.558	0.289	0.212	0.152	0.082	0.057
ASA ($m^2 g^{-1}$)	-	52	40	36	28	23

Table 3. Crystallographic parameters deduced from X-ray diffraction analysis

	CM	CM-1400	CM-1800	CM-2000	CM-2200	CM-2400
d_{002} (nm)	n.d.	n.d.	0.3440	0.3439	0.3447	0.3439
La (nm)	n.d.	n.d.	7.240	7.509	8.315	9.241
Lc (nm)	n.d.	n.d.	2.207	8.229	17.688	19.854

n.d. not determined

List of Figures

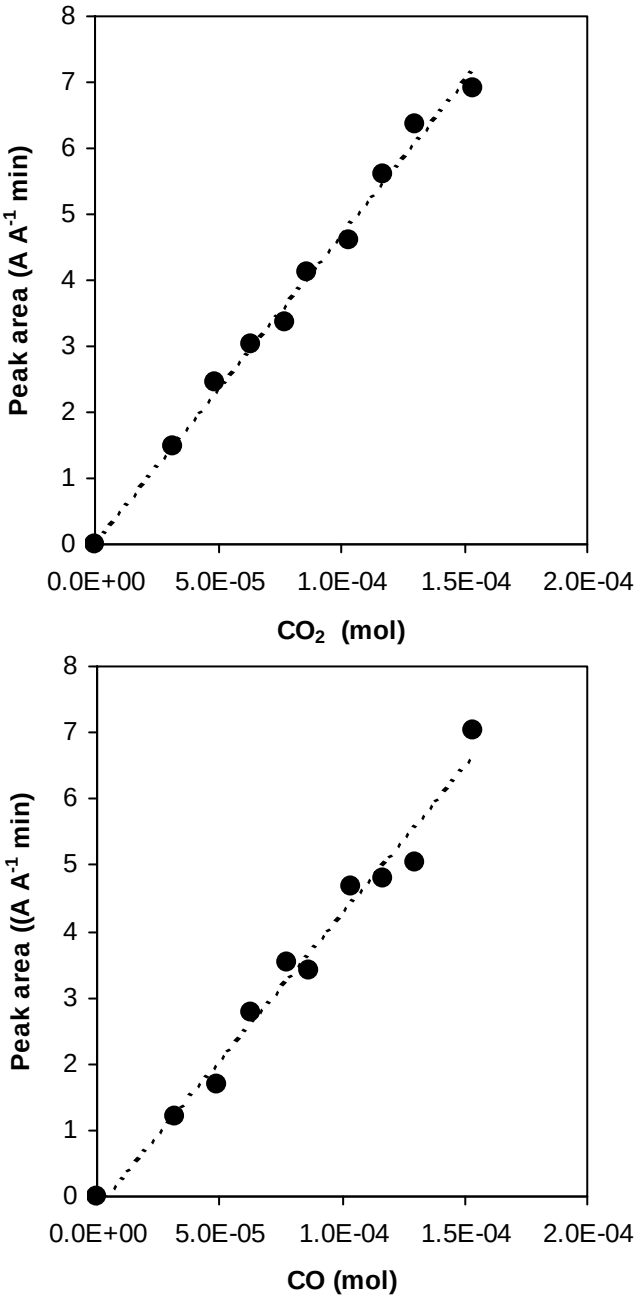

Figure 1
Relationship between structure and reactivity of carbonaceous materials
A. Arenillas et al.

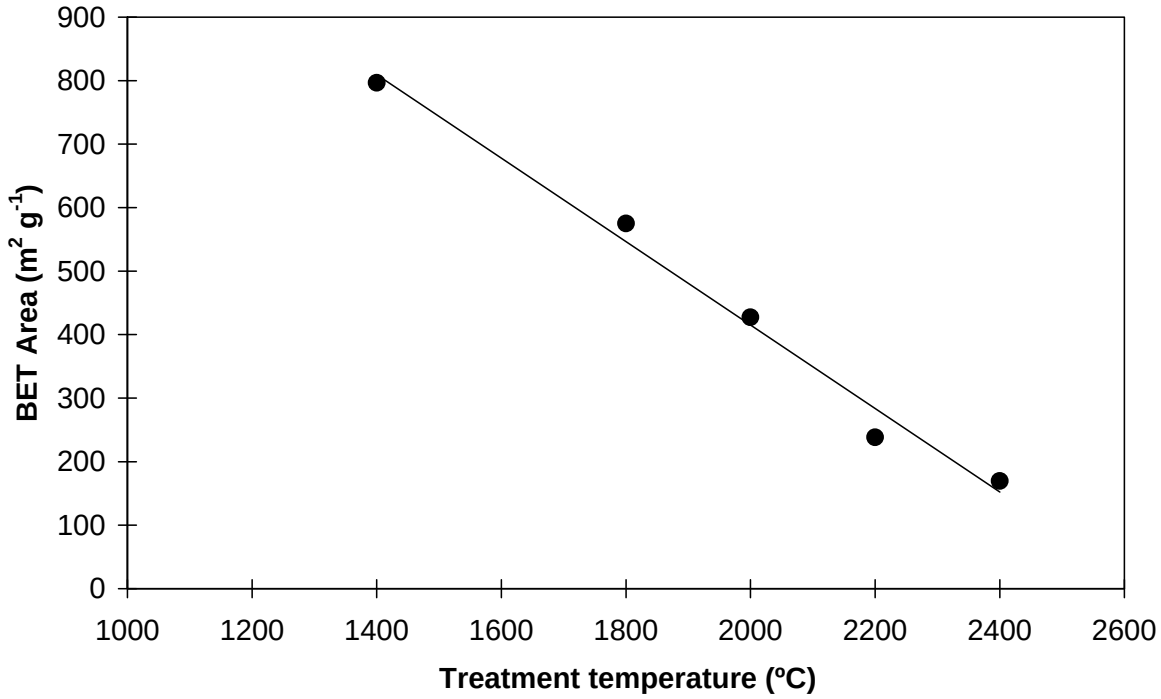

Figure 2
Relationship between structure and reactivity of carbonaceous materials
A. Arenillas et al.

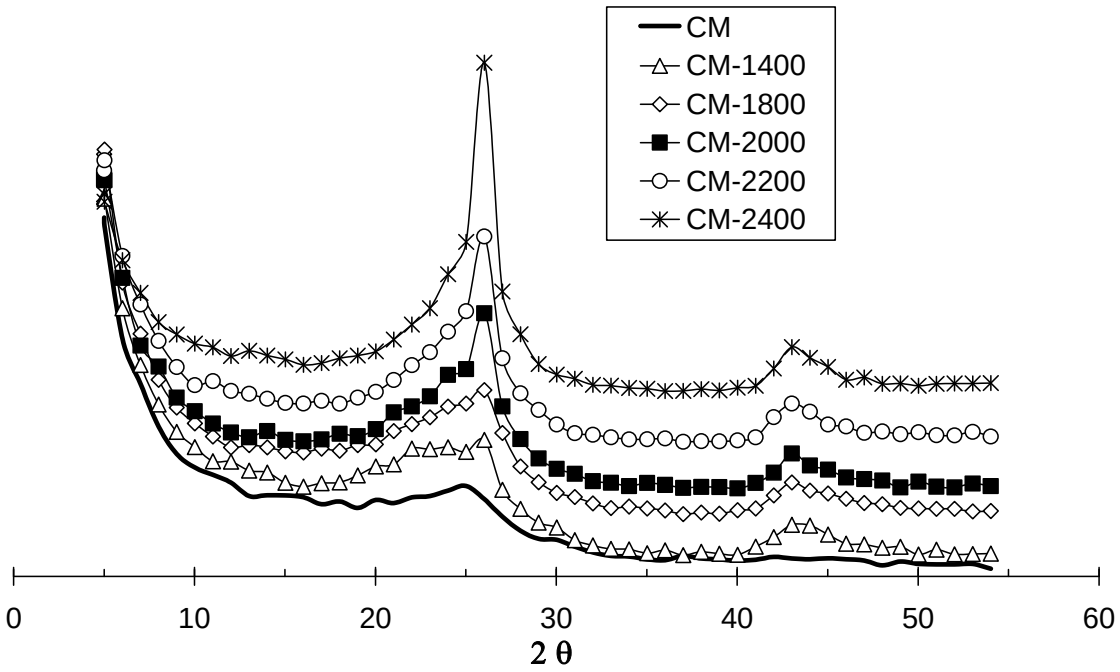

Figure 3
Relationship between structure and reactivity of carbonaceous materials
A. Arenillas et al.

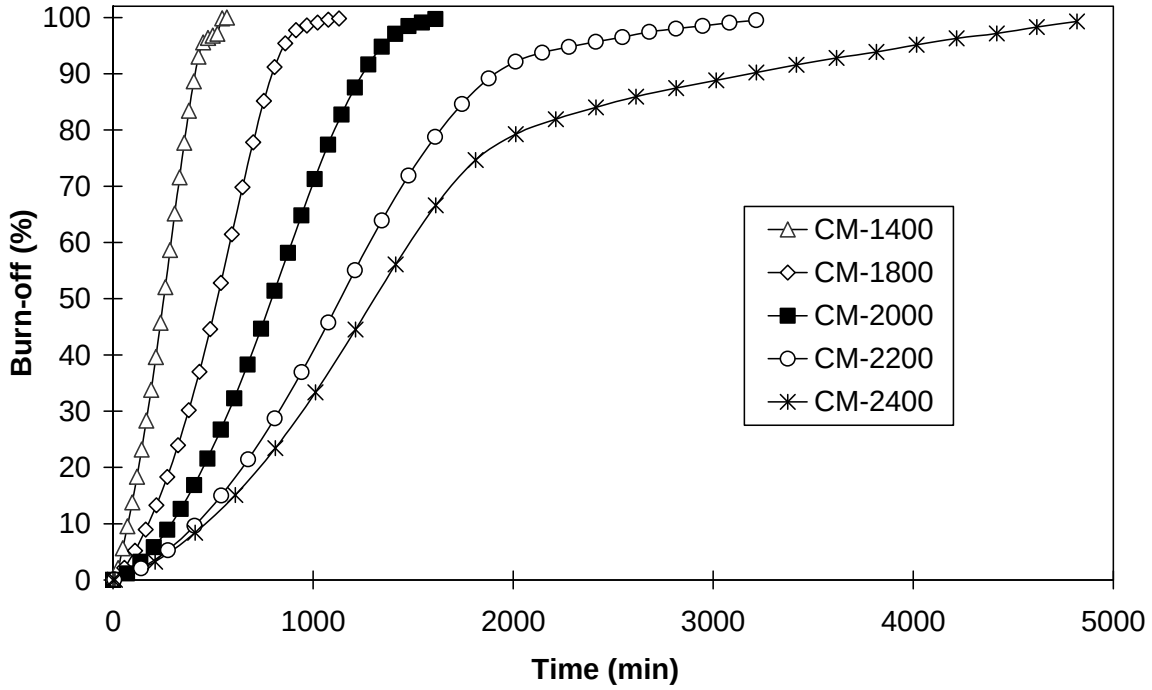

Figure 4
Relationship between structure and reactivity of carbonaceous materials
A. Arenillas et al.

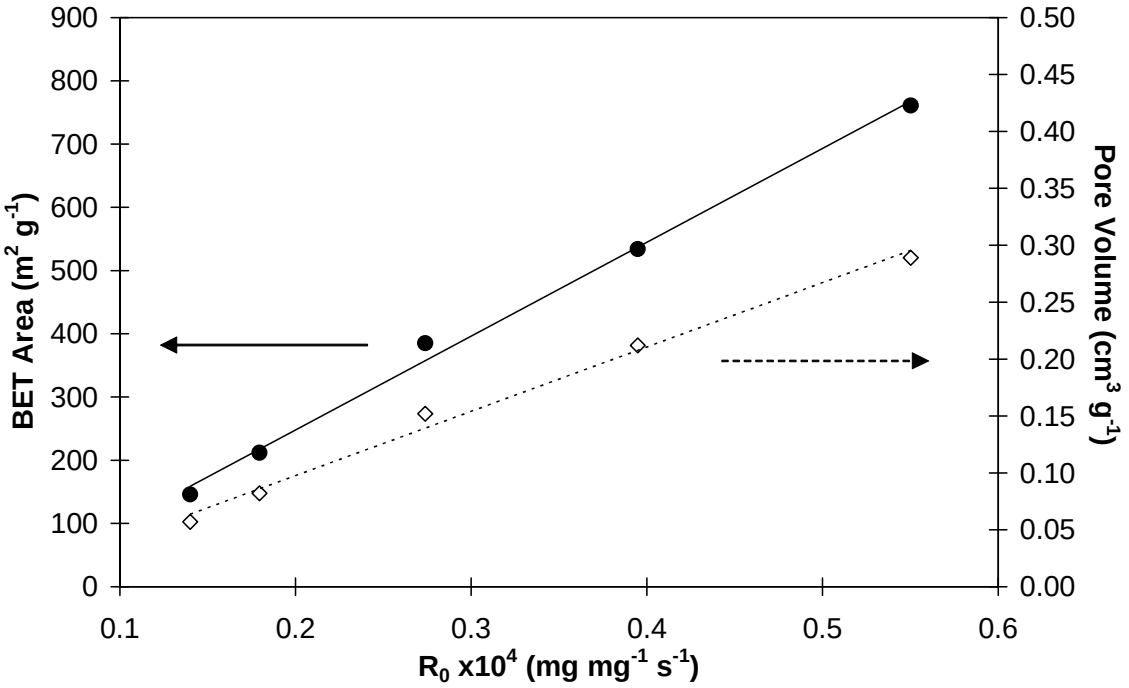

Figure 5
Relationship between structure and reactivity of carbonaceous materials
A. Arenillas et al.

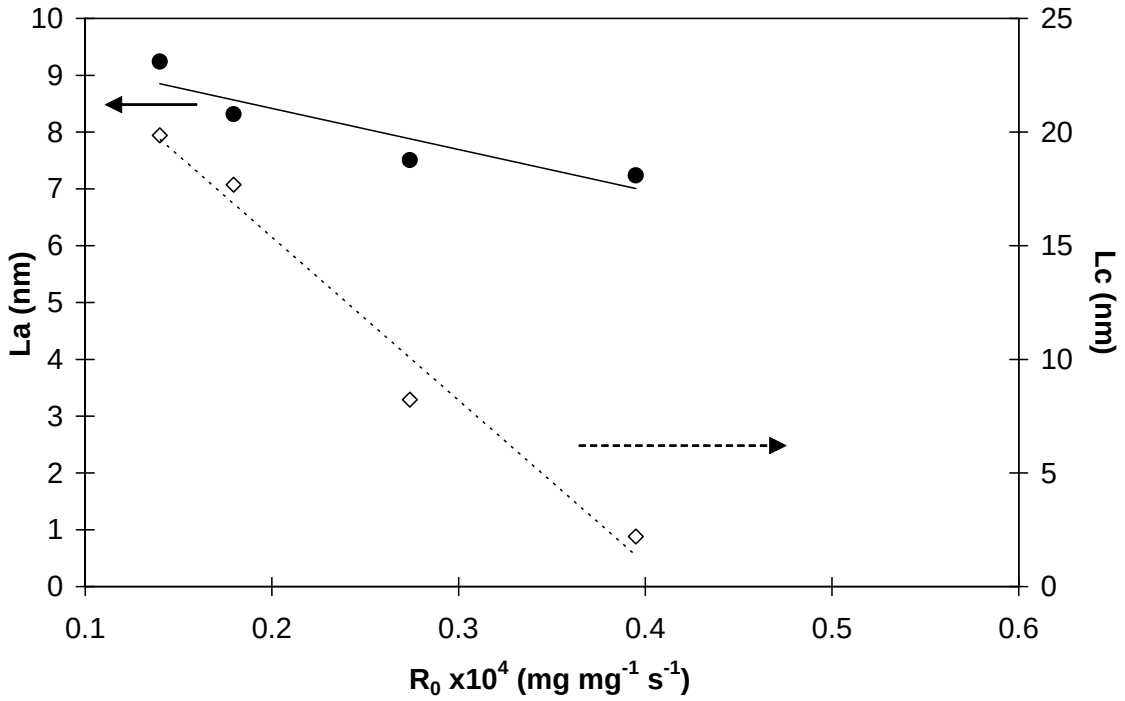

Figure 6
Relationship between structure and reactivity of carbonaceous materials
A. Arenillas et al.

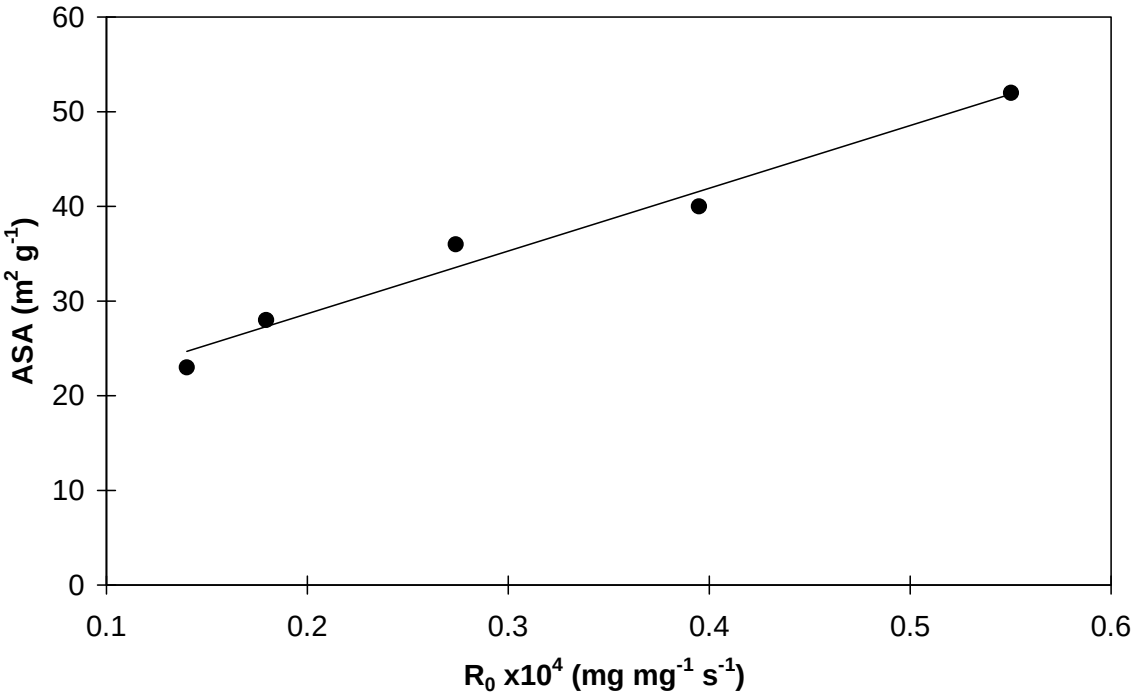

Figure 7
Relationship between structure and reactivity of carbonaceous materials
A. Arenillas et al.

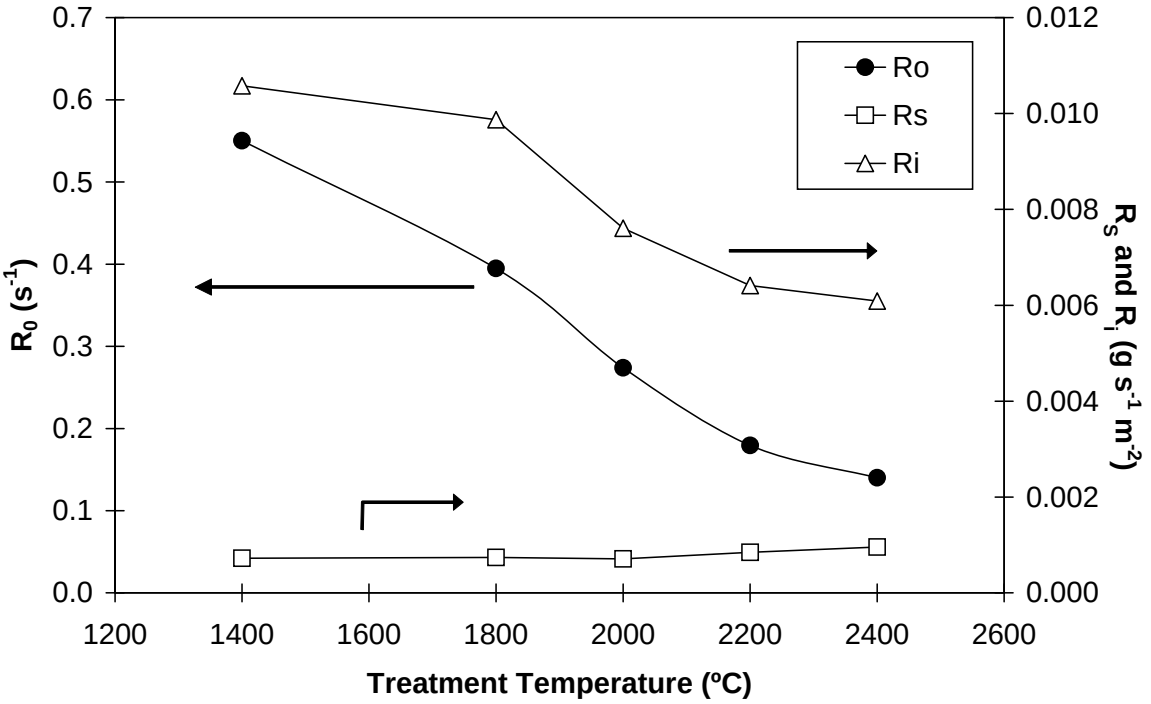

Figure 8
Relationship between structure and reactivity of carbonaceous materials
A. Arenillas et al.